



“Design, Evaluation and Optimization of Novel Topical Drug Delivery System of Antifungal Agent”

Ms. Snehal S. Patil^{1*}, Akshay R. Yadav², Mr. Rohan R. Vakhariya³, Mr. Akash Kere⁴, Dr. Sadik Sayyad⁵, Ms. Shweta Patil⁶

^{1*}Department of Pharmaceutical Chemistry, Krishna Vishwa Vidyapeeth, Krishna Institute of Pharmacy, Karad, Dist. Satara, Maharashtra, India-415539, Email: patilsnehal5121@gmail.com

²Department of Pharmaceutical Chemistry, KCT's Krishna College of Pharmacy, Karad, Dist. Satara, Maharashtra, India- 415539, Email: akshayyadav24197@gmail.com

³Department of Pharmaceutics, Rajarambapu College of Pharmacy, Kasegaon, Dist. Sangli, Maharashtra, India-415404, Email: rohanvakhariya@gmail.com

⁴Department of Pharmaceutics, Amrutvahini College of Pharmacy, Sangamner, Dist. Ahmednagar, Maharashtra, India-422605, Email: akashkere31097@gmail.com

⁵Department of Pharmaceutics, Amrutvahini College of Pharmacy, Sangamner, Dist. Ahmednagar, Maharashtra, India-422605, Email: sfsayyad@amrutpharm.co.in

⁶Department of Pharmacology, Sarojini College of Pharmacy, Kolhapur, Dist. Kolhapur, Maharashtra, India-416003, Email: shwetapatil2298@gmail.com

***Corresponding Author:** Ms. Snehal S. Patil

^{*}Department of Pharmaceutical Chemistry, Krishna Vishwa Vidyapeeth, Krishna Institute of Pharmacy, Karad, Dist. Satara, Maharashtra, India-415539, Email: patilsnehal5121@gmail.com

ABSTRACT:

The core of nanostructured lipid carriers (NLCs), which are colloidal drug delivery systems at the nanoscale, is a lipid mixture made up of both liquid and solid lipids. In contrast to polymeric or metallic nanoparticles, this lipid-based nanosystem is presented as a safe, non-toxic, and biocompatible nano-drug delivery method. Optimizing and characterizing a transdermal drug delivery system loaded with antifungal medications using Nanostructured Lipid Carriers (NLC) is the objective of this work. By extending the drug release via the NLC transdermal gel, this study aims to optimize NLCs and investigate their potential for topical delivery of luliconazole. Pre-formulation studies for the medication and excipients are conducted by IR. To choose appropriate formulation factors from lipids, surfactants, and process variables from ultra-sonication time, pre-optimization experiments were conducted. The solvent diffusion technique was used to design 15 NLC formulations from the variables selected, and the Box-Behnken design using multiple linear regression method (design expert software) was used to optimize the formulations based on the influence of the independent variable on dependent variables such as particle size and percentage entrapment efficiency (% EE). Using the chosen optimal NLC formulation, a transdermal gel was created. Viscosity, drug content, pH, spreadability, and in vitro diffusion experiments were all assessed.

Keywords: Nano-sized, Antifungal, Entrapment efficiency, Drug content.

1. INTRODUCTION:

Due to factors such as decreased solubility, decreased absorption, increased fluctuations in plasma drug concentration, and variations in drug concentration in plasma, as well as food-drug interactions and patient-related factors like improper prescription, noncompliance, and increased toxicity, conventional medication is currently exploring a novel drug delivery system. These factors are crucial in reducing the desired in-vivo pharmacological effect.^{[1][2]} Because of these repercussions, traditional distribution methods failed, opening the door for innovative drug delivery methods such nanostructured lipid carriers (NLC). The solubility and bioavailability of medications in the aforementioned class may be improved by using lipids as a delivery or carrier system for lipophilic, less water-soluble medications (BCS Class II pharmaceuticals like luliconazole).^[2,3] These days, lipid nanoparticles such as NLC have the ability to transport pre-existing lipid particulate systems such polymeric nanoparticles and liposomes.^[4] NLC can be administered via oral, ophthalmic, parenteral, cutaneous, rectal, and pulmonary routes and guarantees good stability both chemically and physically, as well as good drug loading capacity and good release-controlling carriers.^[4-5] NLCs exhibit the following special characteristics. Excellent physiochemical variety in contrast to every other system of lipid carriers, With respect to Solid Lipid Nanoparticles (SLN), good biocompatibility high potential for improving the bioavailability of medications that are not very soluble in water, Excellent target capability through a process of selective lymphatic absorption and The viability of expanding to a large size ^[6,7].

This study set out to determine the best topical formulations of luliconazole that would both reduce skin irritation and increase drug retention in the skin by creating a nanostructured formulation. with the smallest possible



particle size. The solvent diffusion approach was used to generate liconazole-loaded NLC, which is suitable for topical delivery.^[7] Therefore, particle size was used to determine the correlations between the lipid phase concentration, temperature, surfactant concentration, and the ratio of liquid lipid to total lipid, as well as the reactions of particle size and entrapment efficiency.^[8,9] The best-fitting models that were derived yielded the optimal formulations. Finally, the optimized NLC's morphological characteristics were examined.^[5]

2. MATERIAL AND METHOD:

2.1 Drug and excipients:

Compritol® ATO 888, Precirol® ATO 5, and Capryol 90 (Gattefosse, India) were used as solid lipids and as liquid lipids for NLC, respectively. Tween 20 (Merck, Mumbai) and Tween-80 (Merck, Mumbai) were chosen as surfactants, Luliconazole was supplied by Opatrix Laboratories, Hyderabad. Carbopol 934 (S.D. Fine-Chem Pvt. Ltd., Mumbai) was selected as the gel-forming agent. The water used in the experiment was distilled. All other chemicals and solvents were of analytical reagent grade.

2.2 Selection of excipients:

Maximum drug solubility was used to select solid and liquid lipids for NLC synthesis. The drug's solubility in Cetyl Alcohol, Precirol® ATO 5, and Compritol® 888 was evaluated for solid lipids. A glass beaker containing one gram of lipid was placed on a magnetic stirrer at a temperature higher than 10 °C above the lipid melting point. Using tiny increments and continuous stirring, a predetermined amount of medication was added gradually. After every addition, stirring was maintained for 30 minutes to guarantee the drug's full solubility. The mixture was examined for transparency and clarity. The drug's solubility saturation point in the lipid was evaluated by the loss of transparency ^[10].

The drug's solubility in capryol 90 and oleic acid was evaluated in order to choose liquid lipids. Five milliliters of liquid lipid or oil phase were placed in a glass beaker and allowed to sit at room temperature on a magnetic stirrer in order to test the drug's solubility. The oil or liquid lipid was gradually mixed with a carefully weighed quantity of the medicine, and each addition was stirred for 30 minutes. The saturation point was identified by the loss of transparency. To remove the remaining drug, the resulting solution was centrifuged for 15 minutes at 15,000 rpm using a High-speed cooling centrifuge (REMI, C24, India). The supernatant was then carefully collected and examined to determine the drug concentration.

2.3 Screening of surfactant:

The selection of the surfactant was based on how it affected the formulation's stability and size. For screening, a variety of surfactants with different HLB values were used. Measurements were made to see how Tween 20 and Tween 80 affected the size and stability of blank NLC. Phase separation/creaming or floccule formation in the placebo formulation were used to observe stability.

2.4 Experiment design (response surface methodology/Box-Behnken design):

Utilizing Design Expert® (Version 13, State-Ease Inc., USA), experimental design and formulation optimization of the preparation of NLC were conducted utilizing response surface methods, namely the three-level, three-factor Box-Behnken design. The NLC (Luliconazole-loaded nano lipid carrier) was made using a solvent diffusion process in accordance with formulation factors and prior research. NLCs loaded with drugs were created using the solvent diffusion technique. Following lipid screening, Compritol® ATO 888 (melting point: 70 °C) and Capryol 90 were first chosen as solid and liquid lipids, respectively, for the creation of NLC.^[11] The Box-Behnken design was able to optimize the process with the fewest number of runs (15 runs), including three replicated center points, by identifying the best design for assessing the quadratic response surface and second-order polynomial model. (Table 2) A three-factor, three-level design is explained by a computer-generated non-linear, polynomial model quadratic equation, which is provided below^[12].

$$Y = b_0 + b_1A + b_2B + b_3C + b_{12}AB + b_{13}AC + b_{23}BC + b_{11}A^2 + b_{22}B^2 + b_{33}C^2$$

Where X1 to X3 A, B, and C represent the coded levels of prefixed independent variables (X1 stands for Solid: Liquid Lipid Ratio, X2 for Surfactant Concentration, and X3 for Ultrasonication Time, respectively), Y represents the dependent variable, b0 for the intercept, and b1 to b33 indicate the regression coefficient derived from the observations of individual responses. Furthermore, other expressions such as X1 x2, X1 x3, X2 x3, and Xi 2 (i = 1, 2, and 3) represent the interaction of quadratic terms and independent variables, respectively. Table 1 defines the encoded values of several independent and dependent variables as well as their corresponding levels.

2.5 Preparation of luliconazole-loaded nanostructured lipid carrier:

Using a solvent diffusion approach, the NLC (Luliconazole-loaded nano lipid carrier) was created. The Solvent Diffusion Technique was used to produce drug-loaded NLCs. Following lipid screening, Compritol® ATO 888 (melting point: 70 °C) and Capryol 90 were first chosen as solid and liquid lipids, respectively, for the creation



of NLC. To create a transparent lipid phase, the liquid phase was combined and melted at 70°C. After adding the medication to the melted lipid combination until a clear solution was formed, it was fully dissolved in a solution of ethanol (1:1) and acetone (6 ml)^[13,14]. At the same time, tween 20 was added to an aqueous surfactant solution, which was then heated to the same temperature [15]. Then, using a syringe, the hot melted lipid solution was spread out dropwise in the hot surfactant phase while being continuously stirred at 1000 rpm for the allotted 10 minutes.^[4] After that, the resulting emulsion was sonicated for 10 minutes at 40% amplitude using a probe sonicator. The resulting NLC dispersion was chilled and kept in storage^{[17][18]}

Defining different variables and their respective levels of Box-Behnken design for optimization of NLC.		
Variables	Levels	
	-1	0
		+1
Independent Variables		
A liquid to total lipid Ratio (% w/w)	10	40
B = Lipid Phase Conc. (% w/v)	0.1	1
C= Surfactant conc. (%w/v)	1	4
Dependent Variables		
Y ₁ = Particle Size (nm)	Minimum	
Y ₂ = Entrapment Efficiency (%)	Maximum	

Table No. 1: Dependent and independent variables and their levels

2.6 Characterization of CNL:

2.6.1 FTIR:

Drugs and lipids utilized in NLC manufacture were examined for potential interactions and compatibility using FTIR spectroscopic analysis. An FTIR spectrometer (Bruker, Massachusetts, USA) was used to perform the FTIR spectroscopy. Potassium bromide (KBr) was added to a predetermined volume of sample, and FTIR spectra of the pure drug (Iuliconazole), the physical mixture of drug and lipid, and NLC were recorded. Transmission mode was used for the scanning, and wave numbers between 4000 and 400 cm⁻¹ were used.

2.6.2 Particle Size Analysis and PDI:

Using a particle size analyzer (Nanoparticle Analyzer, Horiba), the dynamic light scattering technique was used to evaluate the particle size and polydispersity index (PDI) of the produced NLC formulations. The drug-loaded nanocarriers were diluted with double-distilled water, and the samples were then examined at room temperature (25 °C). Three separate measurements of the diluted samples' particle size and PDI were made, and the average ± standard deviation was used to describe the results.^[19]

2.6.3 Zeta potential:

The physical stability of the colloidal carrier system is shown by the zeta potential, which is the measurement of the electric charge on the nanoparticle's surface. Zetasizer (ZEN3600, Malvern Panalytical Ltd. UK) was used in the electrophoretic light scattering procedure to measure the Zeta potential or surface charge of the produced NLC. To improve signal strength, the samples were diluted with twice as much distilled water prior to analysis. The results were presented as mean ± standard deviation, and the analysis was conducted in triplicate.^{[20][21]}

2.6.4 % Entrapment Efficiency:

The quantity of drug that is successfully entrapped into the nanocarrier system is measured by drug entrapment efficiency. At separate the lipid and aqueous phase, 5.0 ml of each drug-loaded sample was centrifuged using a centrifuge tube (10000 MWCO) in a centrifuge set at 5000 rpm for 30 minutes at 25 °C. After diluting the supernatant with methanol and filtering it through 40µm filter paper, the UV-VIS spectrophotometer was used to measure the sample's absorbance. This is how the trapping efficiency of NLC was determined.^[22]

$$\% \text{ Entrapment Efficiency} = \frac{\text{Total amount of drug} - \text{amount of free drug}}{\text{Total amount of drug}} \times 100$$

2.6.5 In-vitro drug diffusion study:

A dialysis bag (cellulose membrane, MW cutoff 12,400) containing 2.0 ml of the Iuliconazole formulation was placed in a 40 ml release medium in a beaker that was kept at 37°C and 100 rpm. The releasing media, phosphate buffer (PBS, PH 7.4), was examined using spectrophotometry at 299 nm. To keep the sink condition after sampling, 0.5 cc of fresh medium was added to the release medium.



2.7 Preparation of drug-loaded NLC-based gel:

The formula (Table 2) was used to prepare the NLC-based gel. After first dispersing carbopol in purified water, LZ-NLC dispersion and propylene glycol were added to the blank gel using a high-speed stirrer set to 1000 rpm for five minutes. Triethanolamine was used right away to neutralize the NLC-gel until the pH reached 5.0–6.0. At room temperature ($25 \pm 1^\circ\text{C}$), the gel was allowed to equilibrate for 24 hours. Meanwhile, the LZ-carbopol-gel was made using LZ PBS (10.0 mg/ml) [23]

Formulation Composition	LZ NLC Gel (g)
LZ NLC	50
Carbopol 940	0.75
Propylene Glycol	7.5
Triethanolamine	2.5
Water	100

Table No. 2: Composition of LZ NLC gel formulation (%m/m)

2.8 Characterization of Drug loaded NLC based topical gel:

The basic physicochemical parameters were studied for the developed formulation.

A. Physical Appearance, pH, Viscosity, Spreadability:

The color, clarity, homogeneity, and appearance of the created gel formulation were examined visually. A pH meter was used to determine the pH values of the produced gel's 1% aqueous solution. After dissolving 1 gram of gel in 100 milliliters of distilled water, it was left for two hours. The formulation's pH was measured three times, and the average results were computed. All of the prepared gels were placed in beakers beneath the RV-7 spindle, which was operated at 10 rpm in a Brook Field viscometer to determine the viscosity. The slides method was used to assess the gel's spreadability: 1g of gel was placed between the two slides, the pre-weighted plate was placed above the gel, and additional weights were added to the plate until the gel stopped spreading. The final cumulative weight and the total amount of time it took for the gel to spread were measured and recorded, and the mass of the gel and the total weight applied were compared over time.

Spreadability = Mass x Length/ Time

B. Drug Content:

Ten milligrams of drug-loaded NLC-based gel were weighed, combined with phosphate buffer saline (PBS pH 7.4), and the concentration of LZ was measured using spectrophotometry in order to ascertain the drug content of the gel. As a blank, the NLC gel foundation with the same quantity of components but no medication was utilized.

C. In vitro diffusion study:

Ten milligrams of drug-loaded NLC-based gel were weighed, combined with phosphate buffer saline (PBS pH 7.4), and the concentration of LZ was measured using spectrophotometry in order to ascertain the drug content of the gel. As a blank, the NLC gel foundation with the same quantity of components but no medication was utilized.[24]

D. Stability study:

In accordance with ICH recommendations Q1A (R2), an accelerated stability study was carried out by incubating the optimized batch of NCL for three months at both regular ($25 \pm 2^\circ\text{C}$ temperature and $60 \pm 5\%$ RH) and accelerated settings ($40 \pm 2^\circ\text{C}$ temperature and $75 \pm 5\%$ RH). Physical appearance, particle size, and the formulation's percentage entrapment efficiency were used to gauge the stability. At 0 months, 1 month, and 3 months, the effects of temperature and humidity were noted [21]

E. Statistical analysis:

ANOVA was used for the analysis of variants, and Design Expert® (Version 13, State-Ease Inc., Minneapolis, U.S.A.) and DDSolver 1.0 (Microsoft Corp., U.S.A.) were used for statistical analysis of various parameters. All experiments were conducted in triplicate, and the values reported were the average of three measurements with standard deviation (\pm SD). P-value < 0.05 was deemed significant.

3. RESULT AND DISCUSSION:

3.1. Screening of lipid and surfactant:



Compritol® 888 ATO and Capryol 90 were identified as the most appropriate and compatible solid and liquid lipids for the production of drug-loaded NLC after screening of solid and liquid lipids based on compatibility and solubility. The greatest solubility of liconazole was observed in melted Compritol® 888 ATO. The chosen lipids showed the appropriate level of stability. After screening, we determined that Tween 20 was the most appropriate surfactant for the current investigation. The selection of the surfactant was based on its effect on the size and stability of the NLC [25]

3.2 Physicochemical characterization:

3.2.1 FTIR:

To investigate any potential interactions between the medicine (luliconazole) and the lipid utilized in the formulation, FTIR spectra of the pure drug, physical mixture of drug, and excipients were obtained. Figure 1 displays the FTIR spectra of lipid, liconazole, and a combination of liquid lipid and medication. The FTIR spectra of the pure medication are displayed in Fig. 1(a), and they contain all of the distinctive luliconazole peaks, including 3031.21 and 2990.96, which indicate aromatic and aliphatic C-H stretching. The distinctive overlapping stretching S-H, C≡N, C=C alkene, and C-Cl bond were represented by a medium intensity peak at 2823.42 cm⁻¹, 2192.88 cm⁻¹, 1550.99 cm⁻¹, and 756.60 cm⁻¹, respectively.

The FTIR spectra of lipid, or Capryol 90, are displayed in Fig. 1(b). The high-intensity peak at 2926.02 cm⁻¹ and 1727.79 cm⁻¹ respectively, indicate distinctive (C-H) aliphatic and (C=O) stretching. C-O and O-H are represented by the absorption bands at 1168.25 cm⁻¹ and 3425.29 cm⁻¹, respectively. Figure 1 (c) shows that the distinctive C≡N stretching and aromatic C=C stretching vibrations (Luliconazole) were represented by intensity peaks at 2197.32 cm⁻¹ and 1466.61 cm⁻¹, respectively. (C-H) aliphatic stretching is the cause of the peak at 2926.02 cm⁻¹. The C=O group exhibits a distinctive rocking vibration at 1728.37 cm⁻¹. The mixtures' FT-IR values were identical before and after preparation [26].

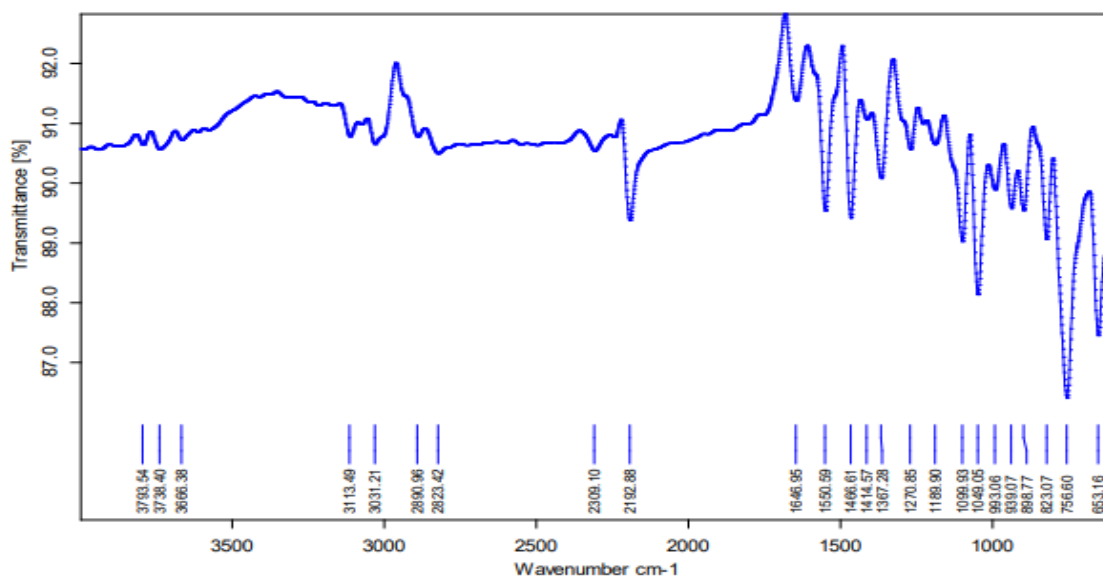


Figure No. 1: FTIR spectra of pure drug luliconazole

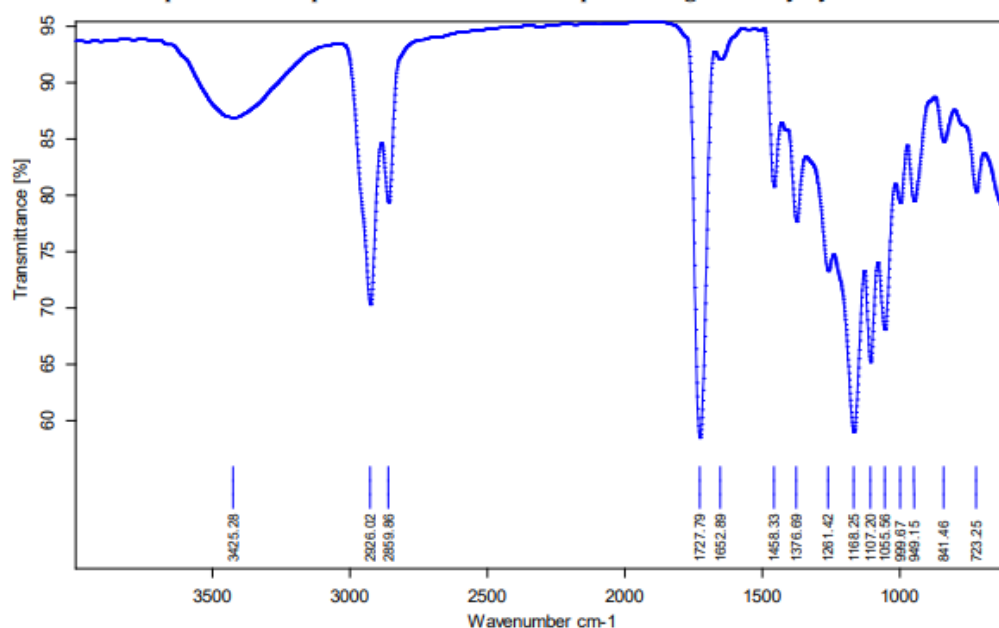


Figure No. 2: FTIR spectra of liquid lipid

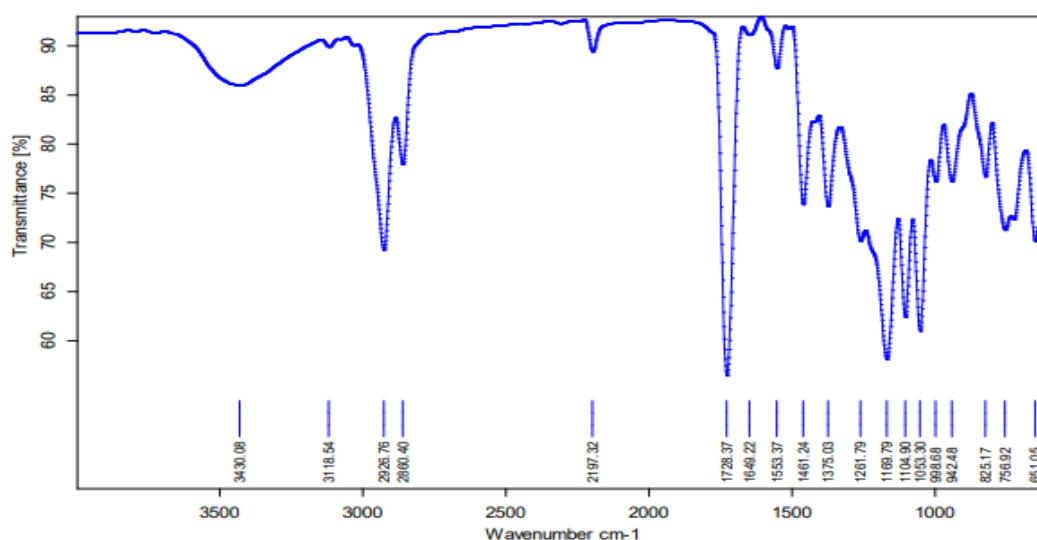


Figure No. 3: FTIR spectra of Physical mixture of drug and lipid.

3.3. Data analysis and formulation optimization:

For process optimization and experimental design, a three-level Box-Behnken design with three factors was employed. 15 runs of various combinations of the selected elements are produced by the response surface randomized design, including 3 runs with center points for which the responses were recorded and examined. Quadratic polynomial models are the particular model terms that were found to provide the greatest fit for all three factors. The dependent variables (responses) were directly impacted by the independent variables, as indicated by the model terms. The optimal experimental parameter was determined by comparing all of the observed responses. In order to forecast the optimal mathematical model and optimum parameters, the answers were analyzed using ANOVA (analysis of variations). The individual and combined factor coefficients and p-values showed how each component affected the chosen responses. The importance of the used model and other factors evaluated by ANOVA were also shown by the P-value (Table 3). For every observed response, lack of fit was not significant, and the model variables were found to be significant as intended. Table 2 displays the experimental design's 15 runs along with each run's corresponding response. Fig. 4 displays the 3D response surface plots of every response that illustrate the impact of many parameters. The following is the final regression equation of the applied quadratic model for individual responses, which includes the drug entrapment efficiency (Y2) and particle size (Y1) generated using the response surface methodology utilizing Design Expert® software.



Impact of different formulation variables (independent parameters) on the response surface methodology-prepared NLC's distinctive features The formulation is optimized using the Box-Behnken design.

Batch Code	Factor A Liquid to total lipid ratio (%w/w)	Factor B Lipid Phase Concentration (%w/v)	Factor C Surfactant Concentration (% w/v)	Response 1 Particle size Y1 (nm)		Response 2 Entrapment Efficiency Y2 (%)	
				Actual	Predicted	Actual	Predicted
F1	40	0.55	4	410.8	393.79	84.6	84.80
F2	25	1	1	695.6	712.71	72.9	73.07
F3	25	0.1	1	482.5	459.21	73.8	73.04
F4	40	0.1	2.5	205.6	218.91	84.4	85.10
F5	10	0.55	4	391.8	358.24	61.7	62.15
F6	10	0.55	1	680.5	649.59	61.5	61.83
F7	25	1	4	632.5	652.26	74.2	74.24
F8	25	0.55	2.5	448.6	480.99	73.1	73.27
F9	25	0.55	2.5	457.8	480.99	73.2	73.27
F10	40	0.55	1	536.7	522.34	84.2	84.28
F11	25	0.1	4	120.4	99.76	73.6	72.72
F12	10	1	2.5	678.3	667.76	63.8	63.33
F13	10	0.1	2.5	310.2	340.06	60.2	60.65
F14	40	1	2.5	724.3	697.21	84.2	83.98
F15	25	0.55	2.5	439.2	480.99	73.6	73.27

Table No. 3: Effect of various formulation variables

Summary of ANOVA and statistical parameters respective to selected responses indicating significance and fitting of different models

Model parameters	fit	Y1: Particle size		Y2: Entrapment Efficiency	
		p-value	Interpretation	p-value	Interpretation
Model		< 0.0001	significant	< 0.0001	significant
R2		0.9795		0.9972	0.9972
R2 _adjusted		0.9641		Adjusted R ²	0.9951
AICc		26.0709		59.8252	
Lack of fit		0.0538	not significant	0.1396	not significant
X1		0.0963		< 0.0001	
X2		< 0.0001		0.1043	
X3		< 0.0001		0.3445	
X1X2		0.0601		0.0131	
X1X3		0.0456		0.8714	
X2X3		0.0025		0.2454	
X1 2					
X2 2					
X3					

Table No. 4: Summary of ANOVA and statistical parameters

$$Y1 = 121.05 + 41.28 \times x1 - 42.32 \times x2 + 0.13 \times x3 + 51.17 \times X1X2 - 18.26 \times X1X3 - 13.58 \times X2X3 + 125.60 \times x1^2 + 107.04 \times x2^2 + 47.87 \times x3^2 \quad (3)$$

$$Y2 = 91.68 + 3.80 \times x1 - 0.62 \times x2 - 3.24 \times x3 + 4.52 \times X1X2 - 2.04 \times X1X3 + 0.68 \times X2X3 - 3.42 \times x1^2 - 8.75 \times x2^2 - 11.18 \times x3^2 \quad (4)$$

The quadratic equation's coefficient and response surface plot showed that the chosen factors had a major effect on the dependent variables (Y1 and Y2). The regression equation's positive and negative signs before each individual term indicated a rise and fall in the reaction to the factors, respectively.

3.3.1 Effect of independent factors on Response Y1 (Particle size):

The generated formulations' particle sizes ranged from 120.4 nm to 695.6 nm, according to the results. According to the regression equation, it was evident that the Lipid Phase Conc (X2) had a direct impact on particle size (Y1), although the surfactant concentration (X3) had an inverse relationship. The Liquid to Total Lipid Ratio (X1), Eq. (3), had no discernible influence. More specific details on how several independent parameters affect particle size may be found in the 3D response surface plot (Fig. 4(A)–(C)). The solid/liquid



lipid ratio (X1) shifted from level -1 to 0 on the graph, indicating an initial drop in particle size. This was followed by a large increase from 0 to + 1.

This reaction could be caused by an early rise in solid lipid, which will create the ideal mixture of liquid and solid lipid, giving NLC the required structure at the smallest size. On the other hand, as the concentration of solid lipids rises further, more solid material accumulates and the particle size increases as well. Furthermore, an increase in surfactant concentration (X3) caused a significant decrease at first, which was followed by a minor increase in particle size as the surfactant concentration increased.^[27] The initial increase in surfactant concentration is supposed to reduce the interfacial tension and create steric hindrance on the NLC surface to prevent the accumulation of individual particles and improve stability. [

^{28]} After the surfactant concentration reaches saturation, more surfactant molecules are deposited on the NLC surface, which again causes a modest increase in size. The three-dimensional picture made it evident that components A and B and A and C work together to influence particle size. The highest level of X2 and X3 was associated with the largest particle size, whereas the center value of all the independent components was associated with the smallest particle size.

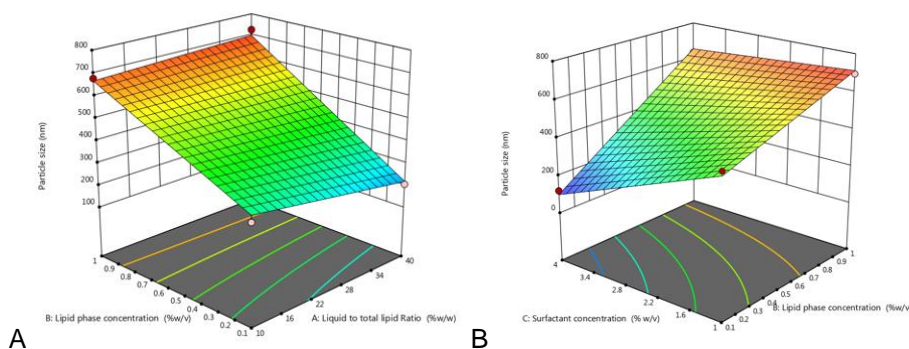
3.3.2 Effect of independent factors on Response Y2 (Entrapment Efficiency):

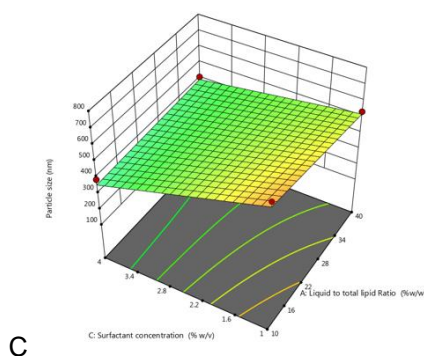
The developed formulations' percentage entrapment efficiency was observed to range from 60.2% to 84.6%. According to the final quadratic equation, the formulation's entrapment effectiveness is inversely proportional to the surfactant concentration and directly related to the lipid ratio (Eq. (4)). The percentage entrapment efficiency increased significantly as the liquid to solid/lipid ratio increased, but then somewhat decreased as the ratio increased further, according to the 3D response surface plot. The reason for this could be because the initial rise in solid lipid content made it easier for the medicine to dissolve (as luliconazole dissolves well in melting Compritol® 888).^[29] Additional lipid ratio increases led to an excessive decrease in liquid lipid content, which reduced the amount of drug entrapment in the liquid compartment of the NLC matrix and encouraged the evacuation of drugs that were already entrapped from the solid matrix. Similarly, a rise in surfactant concentration first produced an entrapment efficiency curve that grew before declining as more improvement was made. A higher concentration of surfactant may improve drug partitioning and make it easier for the drug to dissolve in the lipid and aqueous phases. With a further increase in surfactant, the lipid matrix may become saturated, and drug expulsion from the lipid matrix was found to reduce entrapment efficiency.^[30]

3.3.3 Optimization and point prediction:

The software optimized the prepared formulas following statistical analysis and evaluation of the influence of each individual factor on the answers. In order to accomplish the intended objectives of the chosen replies, optimization provides accurate formulation parameters.^[31] As per desirability, particle size (Y1) was set to minimize, and entrapment efficiency (Y2) was set to maximize. The numerical optimization of the Box-Behnken design suggested the most suitable values of the formulation variables as 40 liquids to total lipid ratio, 0.16 lipid phase concentration, and 4% surfactant concentration. The predicted responses for optimized formulation by Design Expert® were noted as 120.396 nm and 83.351% for particle size and entrapment efficiency. Further, the finally optimized batch was prepared as per the suggested proportion and experimental conditions, which was then subjected to further evaluation.^[21]

Particle Size:





Entrapment Efficiency:

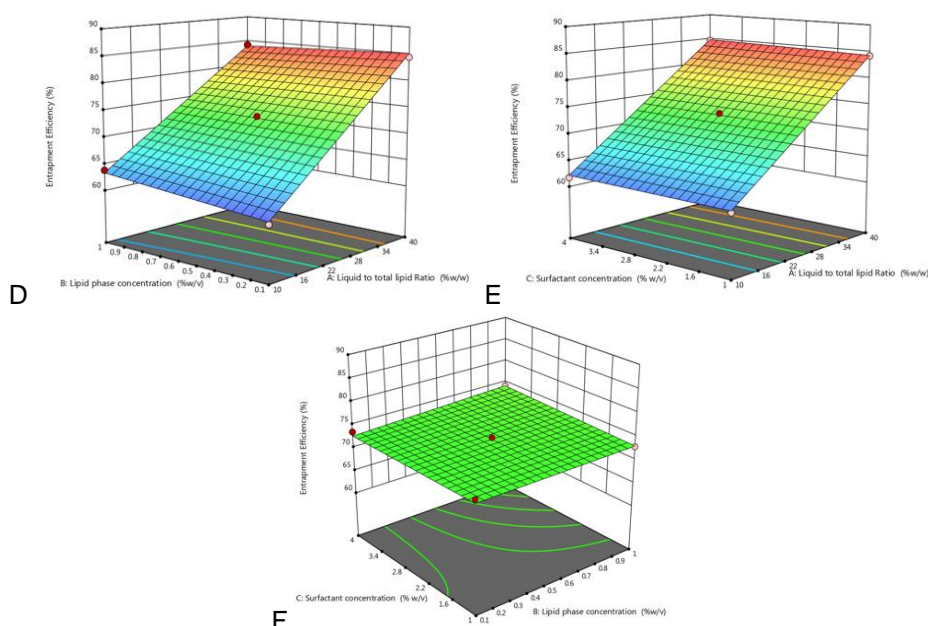


Figure No. 4: 3D-response surface plot for optimization of the prepared formulations, showing the impact of different formulation variables (independent factors) on characteristic features of the developed NLC; (A–C) effect of X1, X2, and X3 and their interaction terms on particle size (Y1); (D–F) effect of X1, X2, and X3 and their interaction terms on entrapment efficiency (Y2).

3.4 Particle size, PDI, and zeta potential:

Zeta Potential, Polydispersity Index (PDI), and particle size measurement: NLC filled with LZ displayed the ideal particle size. This could be the result of the ideal concentration of a lipid and surfactant combination, which works in concert to reduce particle size. Particle size has been found to decrease as surfactant concentration rises; a smaller particle size facilitates drug targeting and enhances drug penetration across biological membranes. [32-34] Permeation through the skin is the primary need for a topical drug delivery system loaded with nanoparticles; in the case of NLC, the particle size should be sufficiently tiny to allow for skin penetration. For the creation of NLC formulation, entrapment efficiency can therefore be disregarded or is viewed as less important than particle size. All formulations had zeta potential values between -16.3 and -17.5 mV. Storage stability, or the ability of the dispersion to withstand aggregation, is conferred by a high zeta potential. [35,36] Zeta potential first rises and then falls, according to research. This could be attributed to Tween 20, a surfactant. Because it is adsorbed on the particle/water interface and forms an electric double layer following ionization in water, an ionic emulsifier has the highest zeta potential. The particle size distribution of nanoparticles is measured by the polydispersity index. Polydispersity values less than 0.5, which denote a uniform dispersion, are found in samples having a broad size distribution. [16] The polydispersity index (PDI) values fall between 0.224 and 0.462. The formulation yielded the PDI's smallest value, 0.224. It has been noted that as solid lipid levels rise, so does the PDI value. [23]

3.5 Entrapment efficiency:



It was discovered that the entrapment efficiency of LZ-loaded NLC ranged from 79.46% w/w to 99.99% w/w. It has been found that entrapment rises in tandem with the concentration of liquid lipid (Capryol). The degree of crystallinity of lipid nanoparticles is always associated with encapsulation efficiency. The encapsulation efficiency increases with the amount of capryol in the mixture. By increasing the amount of amorphous material in the solid lipid matrix, capryol improves the encapsulation efficiency by reducing the total particle crystallinity [37]

3.6 *In vitro* drug release study:

In vitro release investigation of drug-loaded NLCs LZ-loaded NLC demonstrated optimum *in vitro* drug release up to 24 h. The *in vitro* release of the drug from the NLC dispersion was found to be biphasic, with the initial burst effect followed by steady release of the drug [38]

Either the untrapped drug in the NLC dispersion or the location of liquid lipid in the outer shell, which includes lipophilic drug in dissolved form and causes the initial burst release at the initial stage, could be the cause of the initial burst release. Diffusion or matrix erosion can cause release. While sustained release delivers the medication over an extended period of time and maintains therapeutic drug concentration at the site of action, initial burst release gives the drug for rapid therapeutic effect and enhances drug penetration. This suggests that utilizing this formula with a single dose frequency could result in sustained release.

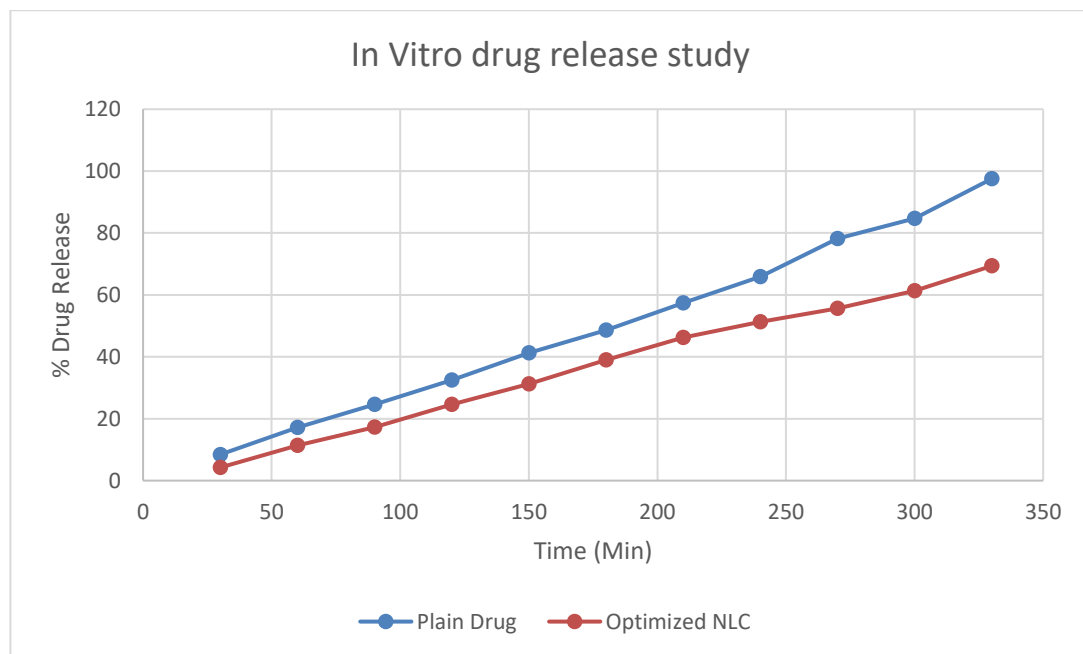


Figure No. 5: In-vitro drug release study

3.7 Characterization of Drug Loaded NLCs Gel:

Following NLC optimization, the gel was formulated using LZ NLCs. Drug-loaded NLC topical gel characteristics: The formulations had a uniform texture, were transparent, and were clear. Formulations with a pH between 7.1 and 7.4 are well accepted on the skin without causing irritation. The viscosity of LZ NLCs is optimal. On application, LZ NLCG spreads rather easily. The results of the diffusion investigation showed that the drug was diffused by the produced NLCs in a regulated manner and that the NLC gel formulation did not cause any drug burst release.

[39]

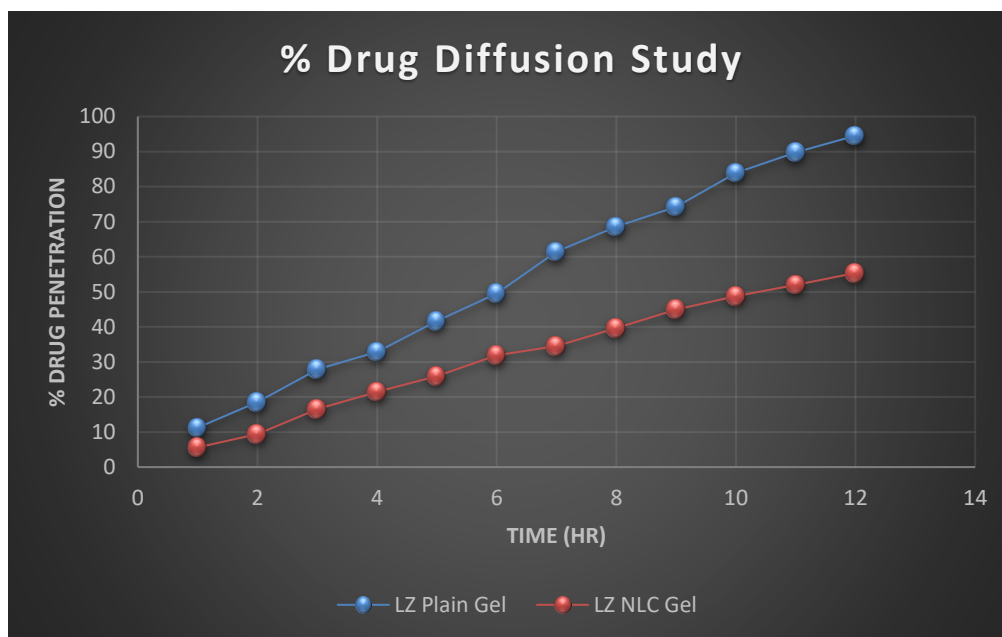


Figure No. 6: % Drug Diffusion of LZ Carbopol Gel and LZ NLC Gel

3.8 Stability studies:

An accelerated stability study of the prepared formulation was performed in terms of physical appearance, particle size, and drug entrapment efficiency upon storage in different conditions as per the ICH guidelines Q1A. The formulation was observed at different time intervals, as mentioned above. (12) No significant change in the physical appearance of the NLC was observed at both the regular and accelerated conditions of temperature and humidity. A small increase in particle size and an a decrease in entrapment efficiency were recorded after 3 months of storage at both conditions. The changes were slightly higher in accelerated conditions than in the regular condition (Table 5). Although the changes were not as significant to be considered and thus it can be concluded that the optimized formulation was satisfactorily stable during the entire period.^[21]

Time (Month)	25 ± 2 °C and 60 ± 5% RH			40 ± 2 °C and 75 ± 5% RH		
	Change in Physical Appearance	Particle size (nm)	% EE	Change in Physical Appearance	Particle size (nm)	% EE
0	No	122.56	84.8	No	122.52	84.8
1	No	122.71	85.24	No	124.93	83.17
3	No	124.78	78.54	No	128.47	76.54

Table No. 5: Accelerated stability study of IN CNL as per ICH guideline.

4. CONCLUSION:

The current work demonstrated that Luliconazole, a poorly soluble medication, could be considerably synthesized in NLC-loaded gels. NLCs filled with drugs could easily heal inflammation. Using Box-Behnken design and response surface approach, experimental design and optimization were carried out. While the gel will hydrate the skin, the lipids used in NLC may have an emollient effect. This allows the drug to be successfully loaded into the gel after being integrated into NLCs. With sustained release, the formulation can be widely used to meet clinical and physiological needs.

The results showed drug penetration, confirming the potential of NLC as carriers for topical delivery. Excellent characterization parameters for particle size, PI, zeta potential, and in vitro release patterns have been demonstrated by licoanazole-loaded NLC. Even if the exact mechanism by which these mechanisms work is yet unknown, the antifungal impact is extended by the presence of nanoparticles containing active medicinal ingredients. There are enough information revealed by this study to demonstrate that dermal delivery has enormous potential for targeted and long-lasting releasing effects.

REFERENCES:

- Garcês A, Amaral MH, Lobo JMS, Silva AC. European Journal of Pharmaceutical Sciences Formulations based on solid lipid nanoparticles (SLN) and nanostructured lipid carriers (NLC) for cutaneous use : A review. Eur J Pharm Sci. 2018;112(November 2017):159–67. 3



2. Huang W, Dou H, Wu H, Sun Z, Wang H, Huang L. Preparation and Characterisation of Nobiletin-Loaded Nanostructured Lipid Carriers. 2017;2017.
3. Iqbal B, Ali J, Baboota S. Silymarin loaded nanostructured lipid carrier: From design and dermatokinetic study to mechanistic analysis of epidermal drug deposition enhancement. Vol. 255, *Journal of Molecular Liquids*. Elsevier B.V; 2018. 513–529 p.
4. Lauterbach A, Müller-goymann CC. *European Journal of Pharmaceutics and Biopharmaceutics* Applications and limitations of lipid nanoparticles in dermal and transdermal drug delivery via the follicular route. *Eur J Pharm Biopharm*. 2015;(July).
5. Sharma G, Thakur K, Raza K, Singh B. Nanostructured Lipid Carriers : A New Paradigm in Topical Delivery for Dermal and Transdermal Applications. 2017;34(4):355–86.
6. Sanad RA, Abdelmalak NS, Tahany S, Badawi AA. Formulation of a Novel Oxybenzone-Loaded Nanostructured Lipid Carriers (NLCs). 2010;11(4):1684–94.
7. Chakraborty S, Shukla D, Mishra B, Singh S. *European Journal of Pharmaceutics and Biopharmaceutics* Lipid – An emerging platform for oral delivery of drugs with poor bioavailability. *Eur J Pharm Biopharm*. 2009;73(1):1–15.
8. Belouqui A, Solinís MA, Delgado A, Évora C, Pozo-rodríguez A, Gascón AR. *European Journal of Pharmaceutics and Biopharmaceutics* Biodistribution of Nanostructured Lipid Carriers (NLCs) after intravenous administration to rats: Influence of technological factors. *Eur J Pharm Biopharm*. 2013;(February).
9. Iqbal MA, Md S, Sahni JK, Baboota S, Dang S, Ali J. Nanostructured lipid carriers system: Recent advances in drug delivery. *J Drug Target*. 2012;20(10):813–30.
10. Firdaus S, Hassan N, Mirza MA, Ara T, El-Serehy HA, Al-Misned FA, et al. FbD directed fabrication and investigation of luliconazole based SLN gel for the amelioration of candidal vulvovaginitis: a 2 T (thermosensitive & transvaginal) approach. *Saudi J Biol Sci*. 2021;28(1):317–26.
11. Ahad A, Aqil M, Kohli K, Sultana Y, Mujeeb M, Ali A. Formulation and optimization of nanotransfersomes using experimental design technique for accentuated transdermal delivery of valsartan. *Nanomedicine Nanotechnology, Biol Med*. 2012;8(2):237–49.
12. Khan AA, Mudassir J, Akhtar S, Murugaiyah V, Darwis Y. Freeze-dried lopinavir-loaded nanostructured lipid carriers for enhanced cellular uptake and bioavailability: Statistical optimization, in vitro and in vivo evaluations. *Pharmaceutics*. 2019;11(2):1–19.
13. Hu FQ, Jiang SP, Du YZ, Yuan H, Ye YQ, Zeng S. Preparation and characterization of stearic acid nanostructured lipid carriers by solvent diffusion method in an aqueous system. *Colloids Surfaces B Biointerfaces*. 2005;45(3–4):167–73.
14. Kumar M, Shanthi N, Mahato AK, Soni S, Rajnikanth PS. Preparation of luliconazole nanocrystals loaded hydrogel for improvement of dissolution and antifungal activity. *Heliyon [Internet]*. 2019;5(5):e01688.
15. Dudhipala N, AY AA. Amelioration of ketoconazole in lipid nanoparticles for enhanced antifungal activity and bioavailability through oral administration for management of fungal infections. *Chem Phys Lipids*. 2020;232(June):104953.
16. Hejri A, Khosravi A, Gharanjig K, Hejazi M. Optimisation of the formulation of β -carotene loaded nanostructured lipid carriers prepared by solvent diffusion method. *Food Chem*. 2013;141(1):117–23.
17. Baghel S, Nair VS, Pirani A, Sravani AB, Bhemisetty B, Ananthamurthy K, et al. Luliconazole-loaded nanostructured lipid carriers for topical treatment of superficial Tinea infections. Vol. 33, *Dermatologic Therapy*. 2020.
18. Rapalli VK, Kaul V, Waghule T, Gorantla S, Sharma S, Roy A, et al. Curcumin loaded nanostructured lipid carriers for enhanced skin retained topical delivery: optimization, scale-up, in-vitro characterization and assessment of ex-vivo skin deposition. *Eur J Pharm Sci*. 2020;152:105438.
19. Zheng D, Dai W, Zhang D, Duan C, Jia L, Liu Y, et al. In vivo studies on the oridonin-loaded nanostructured lipid carriers. *Drug Deliv*. 2012;19(6):286–91.
20. Luan J, Zhang D, Hao L, Li C, Qi L, Guo H, et al. Design and characterization of Amoitone B-loaded nanostructured lipid carriers for controlled drug release. *Drug Deliv*. 2013;20(8):324–30.
21. Agrawal M, Saraf S, Pradhan M, Patel RJ, Singhvi G, Ajazuddin, et al. Design and optimization of curcumin loaded nano lipid carrier system using Box-Behnken design. *Biomed Pharmacother*. 2021;141(July):111919.
22. Rajinikanth PS, Chellian J. Development and evaluation of nanostructured lipid carrier-based hydrogel for topical delivery of 5-fluorouracil. *Int J Nanomedicine*. 2016;11:5067–77.
23. Han F, Yin R, Che X, Yuan J, Cui Y, Yin H, et al. Nanostructured lipid carriers (NLC) based topical gel of flurbiprofen: Design, characterization and in vivo evaluation. *Int J Pharm*. 2012;439(1–2):349–57.
24. Gönüllü Ü, Üner M, Yener G, Karaman EF, Aydoğmuş Z, Müller RH, et al. Solid lipid nanoparticles (SLN) and nanostructured lipid carriers (NLC) in cosmetic and dermatological preparations. *Acta Pharm*. 2015;65(1):1–13.



25. Bahari LAS, Hamishehkar H. The impact of variables on particle size of solid lipid nanoparticles and nanostructured lipid carriers; A comparative literature review. *Adv Pharm Bull.* 2016;6(2):143–51.
26. Doktorovova S, Souto EB. Nanostructured lipid carrier-based hydrogel formulations for drug delivery: A comprehensive review. *Expert Opin Drug Deliv.* 2009;6(2):165–76.
27. Sagatova AA, Keniya M V., Wilson RK, Monk BC, Tyndall JDA. Structural insights into binding of the antifungal drug fluconazole to *Saccharomyces cerevisiae* lanosterol 14 α -demethylase. *Antimicrob Agents Chemother.* 2015;59(8):4982–9.
28. Ammar HO, Ghorab MM, Mostafa DM, Abd El-Alim SH, Kassem AA, Salah S, et al. Development of folic acid-loaded nanostructured lipid carriers for topical delivery: preparation, characterization and ex vivo investigation. *J Microencapsul.* 2020;37(5):366–83.
29. Zhao XL, Yang CR, Yang KL, Li KX, Hu HY, Chen DW. Preparation and characterization of nanostructured lipid carriers loaded with traditional Chinese medicine, zedoary turmeric oil. *Drug Dev Ind Pharm.* 2010;36(7):773–80.
30. Kimaro E, Tibalinda P, Shedafa R, Temu M, Kaale E. Formulation development of chewable albendazole tablets with improved dissolution rate. *Heliyon.* 2019;5(12):e02911.
31. Chen N, Chen Y, Tang Y, Zhao Q, Liu C, Niu W, et al. Efficient synthesis of (S)-2-chloro-1-(2, 4-chlorophenyl) ethanol using a tetrad mutant alcohol dehydrogenase from *Lactobacillus kefir*. *Process Biochem.* 2019;85(June):78–83.
32. Souto EB, Müller RH. SLN and NLC for topical delivery of ketoconazole. *J Microencapsul.* 2005;22(5):501–10.
33. Ricci M, Puglia C, Bonina F, Di Giovanni C, Giovagnoli S, Rossi C. Evaluation of indomethacin percutaneous absorption from nanostructured lipid carriers (NLC): In vitro and in vivo studies. *J Pharm Sci.* 2005;94(5):1149–59.
34. Wu P, Huang Y, Chang JJ, Chang J, Tsai Y. Evaluation of pharmacokinetics and pharmacodynamics of captopril from transdermal hydrophilic gels in normotensive rabbits and spontaneously hypertensive rats. 2000;209:87–94.
35. Zhang J, Fan Y, Smith E. PHARMACEUTICAL NANOTECHNOLOGY Experimental Design for the Optimization of Lipid Nanoparticles. 2009;98(5):1813–9.
36. Guo R, Du X, Zhang R, Deng L, Dong A, Zhang J. European Journal of Pharmaceutics and Biopharmaceutics Bioadhesive film formed from a novel organic-inorganic hybrid gel for transdermal drug delivery system. *Eur J Pharm Biopharm.* 2011;79(3):574–83.
37. Dubey A, Prabhu P, Kamath J V. Nano-Structured lipid carriers : A Novel Topical drug delivery system. 2012;4(2):705–14.
38. Souto EB, Müller RH. Lipid nanoparticles: Effect on bioavailability and pharmacokinetic changes. *Handb Exp Pharmacol.* 2010;197:115–41.
39. Joshi M, Patravale V. Formulation and evaluation of nanostructured lipid carrier (NLC)-based gel of valdecoxib. *Drug Dev Ind Pharm.* 2006;32(8):911–8.